

Superconductivity, charge- or spin-density wave, and metal-nonmetal transition in $\text{BaTi}_2(\text{Sb}_{1-x}\text{Bi}_x)_2\text{O}$

Hui-Fei Zhai,¹ Wen-He Jiao,¹ Yun-Lei Sun,¹ Jin-Ke Bao,¹ Hao Jiang,¹ Xiao-Jun Yang,¹ Zhang-Tu Tang,¹ Qian Tao,¹ Xiao-Feng Xu,² Yu-Ke Li,² Chao Cao,² Jian-Hui Dai,² Zhu-An Xu,¹ and Guang-Han Cao^{1,*}

¹Department of Physics, State Key Lab of Silicon Materials, and Center for Correlated Matter, Zhejiang University, Hangzhou 310027, China

²Condensed Matter Physics Group, Department of Physics, Hangzhou Normal University, Hangzhou 310036, China

(Received 10 November 2012; revised manuscript received 25 February 2013; published 8 March 2013)

We have performed an isovalent substitution study in a layered titanium oxypnictide system $\text{BaTi}_2(\text{Sb}_{1-x}\text{Bi}_x)_2\text{O}$ ($0 \leq x \leq 0.40$) by measurements of x-ray diffraction, electrical resistivity, and magnetic susceptibility. The parent compound $\text{BaTi}_2\text{Sb}_2\text{O}$ is confirmed to exhibit superconductivity at 1.5 K as well as charge- or spin-density wave (CDW/SDW) ordering below 55 K. With the partial substitution of Sb by Bi, the lattice parameters a , c , and c/a all increase monotonically, indicating a negative chemical pressure and lattice distortion for the (super)conducting $\text{Ti}_2\text{Sb}_2\text{O}$ layers. Bi doping elevates the superconducting transition temperature to its maximum $T_c = 3.7$ K at $x = 0.17$, and then T_c decreases gradually with further Bi doping. A metal-to-nonmetal transition takes place around $x = 0.3$, and superconductivity at ~ 1 K survives on the nonmetal side. The CDW/SDW anomaly, in comparison, is rapidly suppressed by Bi doping, and vanishes for $x \geq 0.17$. The results are discussed in terms of negative chemical pressure and the disorder effect.

DOI: 10.1103/PhysRevB.87.100502

PACS number(s): 74.70.Xa, 74.62.-c, 71.45.Lr, 75.30.Fv

Superconductivity (SC) and charge- or spin-density wave (CDW/SDW, or abbreviated as DW) are different collective electronic phenomena in crystalline materials. The DW state often appears in low dimensional metallic systems in which the Fermi surfaces (FSs) are nested, showing a real-space modulation of charges or spins. SC can be regarded as another kind of FS instability due to Cooper pairing, which exhibits an electronic ordering in momentum space in the form of condensation of Cooper pairs. While SC generally competes with DW, the coexistence of SC and DW is possible.¹ In iron-based superconducting systems, SC emerges from,² or may also coexist with,³ an antiferromagnetic SDW state, which has aroused enormous and intensive research efforts.⁴

A possible CDW/SDW anomaly has been observed in a class of titanium oxypnictides since the 1990's.^{5–11} The material contains a Ti_2O square lattice that was considered to play an important role for the anomaly.^{12–14} The Ti_2O sheets can be viewed as an analog of the CuO_2 planes in cuprate superconductors (if the Cu and O atoms of the latter are replaced by O and Ti, respectively, Ti_2O lattice forms). Besides, the Ti valence is $3+$, giving a d^1 configuration for Ti^{3+} , in contrast with the d^9 configuration for Cu^{2+} in cuprates. Therefore, continuous efforts have been made to explore possible SC in these layered titanium oxypnictides.^{5,8–10} But it was not until very recently that SC was observed in the related systems. Sun *et al.*¹⁵ observed SC at 21 K and a DW anomaly at 125 K in an intergrowth compound $\text{Ba}_2\text{Ti}_2\text{Fe}_2\text{As}_4\text{O}$ containing both Fe_2As_2 and Ti_2O layers. However, the SC was believed to stem from the Fe_2As_2 layers rather than the Ti_2O sheets. Very recently, Yajima *et al.*¹⁶ reported SC at 1.2 K as well as a DW transition at 50 K in $\text{BaTi}_2\text{Sb}_2\text{O}$. Doan *et al.*¹⁷ found that, by hole doping with sodium, the superconducting transition temperature T_c increased to 5.5 K. Meanwhile the DW transition temperature T_{DW} decreased to about 30 K. The result suggests a competing interplay between SC and the DW ordering.

These findings above call for an investigation of the nature of the DW state and its relation to SC. An earlier neutron diffraction study of $\text{Na}_2\text{Ti}_2\text{Sb}_2\text{O}$ (Ref. 18) failed to observe any long-range magnetic ordering associated with the resistivity anomaly at 120 K. Instead, only a structural distortion in the $\text{Ti}_2\text{Sb}_2\text{O}$ layer was found. On the other hand, theoretical calculations^{12,13} suggest nearly two-dimensional FS nesting that points to a DW instability. Recent first-principles calculations tend to favor SDW scenarios in $\text{BaTi}_2\text{As}_2\text{O}$,¹⁹ $\text{Ba}_2\text{Ti}_2\text{Fe}_2\text{As}_4\text{O}$,¹⁹ $\text{BaTi}_2\text{Sb}_2\text{O}$,²⁰ $\text{Na}_2\text{Ti}_2\text{As}_2\text{O}$,²¹ and $\text{Na}_2\text{Ti}_2\text{Sb}_2\text{O}$.²¹ If the SC is in proximity to an SDW phase, unconventional SC mediated by spin fluctuations could be expected.²⁰ Nevertheless, a CDW instability was also supported by the calculations of phonon dispersions and electron-phonon coupling for $\text{BaTi}_2\text{Sb}_2\text{O}$.²²

Previous reports^{7,9,11,16,17} suggest that T_{DW} decreases remarkably when As^{3-} is replaced by Sb^{3-} , accompanying a lattice expansion. SC appears as the DW is sufficiently suppressed.^{16,17} Therefore, it is of great interest to investigate the effect of isovalent substitution by the last pnictogen Bi in $\text{BaTi}_2\text{Sb}_2\text{O}$.²³ In this Rapid Communication, we present a systematic Bi-substitution study in the $\text{BaTi}_2(\text{Sb}_{1-x}\text{Bi}_x)_2\text{O}$ (1221) system. As expected, the lattice is expanded by the partial substitution. T_c increases up to 3.7 K at $x = 0.17$, and concomitantly the DW anomaly is suppressed. Surprisingly, a metal-to-nonmetal transition takes place around $x = 0.3$ where SC is still robust. The results suggest that the negative chemical pressure suppresses the DW and enhances SC, and the concomitant disorder tends to destroy both the DW and SC in $\text{BaTi}_2(\text{Sb}_{1-x}\text{Bi}_x)_2\text{O}$.

Polycrystalline samples of $\text{BaTi}_2(\text{Sb}_{1-x'}\text{Bi}_{x'})_2\text{O}$ with a nominal Bi content $x' = 0, 0.05, 0.1, 0.15, 0.2, 0.25, 0.3, 0.35, 0.4, 0.45$, and 0.5 were synthesized by a solid state reaction in vacuum using the starting material of powders of BaO (Alfa Aesar, 99.5%), Ti (Alfa Aesar, 99.9%), Sb (Alfa Aesar, 99.5%), and Bi (Alfa Aesar, 99.5%). To obtain a dense pellet that favors the subsequent resistance measurement, intermediate

products of “Ti₂Sb₃” and TiBi were prepared, respectively, at 923 K in an evacuated quartz tube for 24 h. Then the stoichiometric mixtures of BaTi₂(Sb_{1-x}Bi_x)₂O were ground in an agate mortar, and pressed into pellets under a pressure of 2000 kg/cm², in a glove box filled with pure argon (the water and oxygen content was below 0.1 ppm). The pellets, wrapped with Ta foils, were sintered at 1323 K for 30 h in a sealed evacuated quartz ampoule, followed by naturally cooling to room temperature. The as-prepared pellets were very sensitive to moist air. Exposure in ambient conditions for a few hours led to complete decomposition of the 1221 phase.

Powder x-ray diffraction (XRD) was carried out at room temperature using a PANalytical x-ray diffractometer (Model EMPYREAN) with a monochromatic Cu $K\alpha_1$ radiation. The lattice parameters were obtained by least-squares fit of more than 20 XRD reflections with a correction of the zero shift, using a space group of $P4/mmm$ as previously proposed.^{10,16,17} Energy dispersive x-ray spectroscopy (EDXS) on a single crystalline grain under a field-emission scanning electron microscope was used to determine the exact composition, especially for the incorporated Bi content. The measurement precision was within $\pm 5\%$ for the elements Ba, Ti, Sb, and Bi.

Temperature-dependent resistivity was measured in a Cryogenic Mini-CFM measurement system by a standard four-terminal method. Additional resistivity measurements down to 0.5 K were carried out in a ³He refrigerator inserted in a Quantum Design PPMS-9 instrument. Gold wires were attached onto the samples’ newly abraded surfaces with silver paint, keeping the least exposure in air. The size of the contact pads leads to a total uncertainty in the absolute values of resistivity of $\pm 15\%$. Temperature-dependent dc magnetic susceptibility was performed on Quantum Design MPMS-5 equipment. Both the zero-field-cooling (ZFC) and field-cooling (FC) protocols were employed under a field of 10 Oe for probing the superconducting transitions. A magnetic field of $H = 10$ kOe was applied for tracking the DW anomaly.

Samples of BaTi₂(Sb_{1-x}Bi_x)₂O were first characterized by powder XRD. Most of the XRD reflections can be well indexed by a tetragonal lattice, as depicted in the inset of Fig. 1(a), with $a \sim 4.11$ Å and $c \sim 8.10$ – 8.20 Å. Tiny metal Bi was segregated from the main 1221 phase for low-doping ($x' \leq 0.2$) samples, and the amount of Bi and BaTiO₃ impurities increases a little for the high-doping samples. With the Bi doping, the XRD peaks shift systematically [Fig. 1(b)], suggesting that most bismuth incorporates the lattice. The actual Bi content (x) in the 1221 phase was determined by EDXS, which showed nearly 20% less than the nominal value x' , depending on the doping levels and synthetic conditions. The result gives $x = 0, 0.04, 0.08, 0.13, 0.17, 0.20, 0.25, 0.3, 0.35$, and 0.40 for the nominal x' values of $0, 0.05, 0.1, 0.15, 0.2, 0.25, 0.3, 0.35, 0.4$, and 0.45 , respectively.

With the Bi substitution, the (200) reflections move minutely, but the (004) reflections shift remarkably, to the lower diffraction angles, consistent with the mild increase in the a axis, yet with a significant increase in the c axis [Fig. 1(c)]. The lattice expansion indicates a negative chemical pressure by the Bi substitution. Besides, the increase in the c/a ratio suggests structural distortions in the Ti₂Sb₂O layers. It was found that the fractional coordinate of each atom in the unit cell of Na₂Ti₂Sb₂O did not change with the lattice

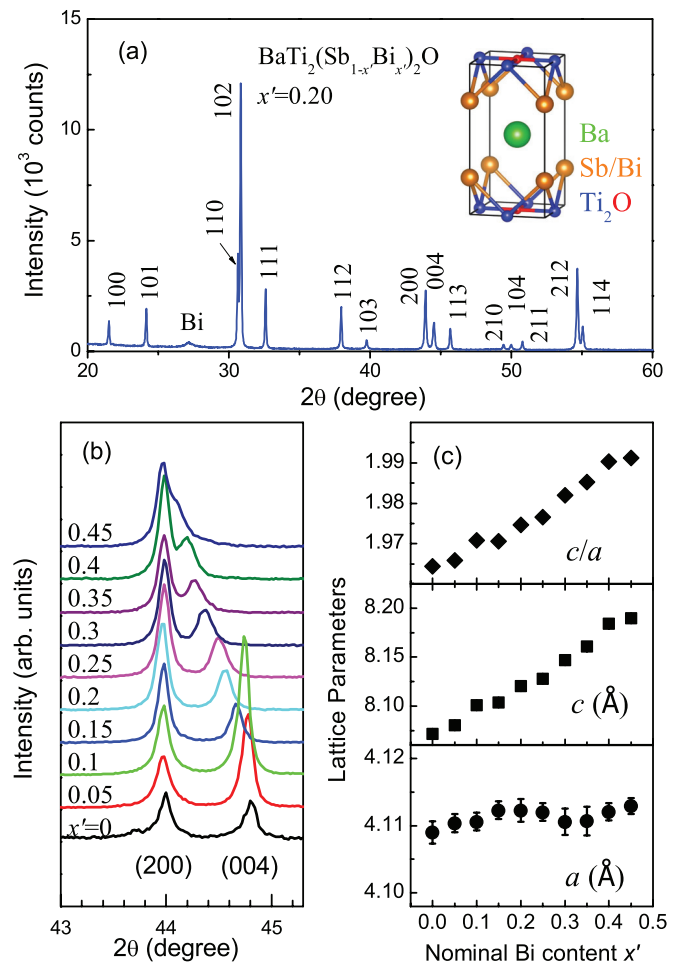


FIG. 1. (Color online) Structural characterizations of BaTi₂(Sb_{1-x}Bi_x)₂O by x-ray diffraction with Cu $K\alpha_1$ radiation. (a) A typical XRD pattern of a $x' = 0.20$ sample indexed by the unit cell is shown in the inset. (b) An expanded plot showing a systematic shift of (200) and (004) reflections with Bi doping. (c) Lattice parameters as functions of nominal Bi content x' .

constants upon decreasing temperature.¹⁸ This means that the c/a ratio is basically proportional to the ratio of the Sb height to Ti-O bond length. The latter influences the crystal field splitting of the Ti 3d orbitals that was linked with the DW instability.¹³ Since the c/a ratio is significantly smaller for a DW state,¹⁸ and furthermore the c/a value is only 1.8 for BaTi₂As₂O whose T_{DW} is as high as 200 K,¹⁰ the increase in c/a would be unfavorable for DW formation. As will be seen below, the DW ordering is indeed suppressed by Bi doping.

Figure 2 shows the temperature dependence of the resistivity [$\rho(T)$] of the BaTi₂(Sb_{1-x}Bi_x)₂O polycrystalline samples. The $\rho(T)$ data of the undoped compound resemble those of previous reports^{16,17} with regard to the DW anomaly at $T_{DW} \sim 55$ K, but the absolute resistivity is about one order of magnitude smaller. The residual resistance ratio (RRR), conventionally defined by the ratio of room-temperature resistance and the low-temperature one, is ~ 20 , much higher than those of previous reports.^{16,17} This suggests the high quality of the present samples. Upon Bi doping, T_{DW} decreases monotonically, and it vanishes for $x \geq 0.17$. As stated above,

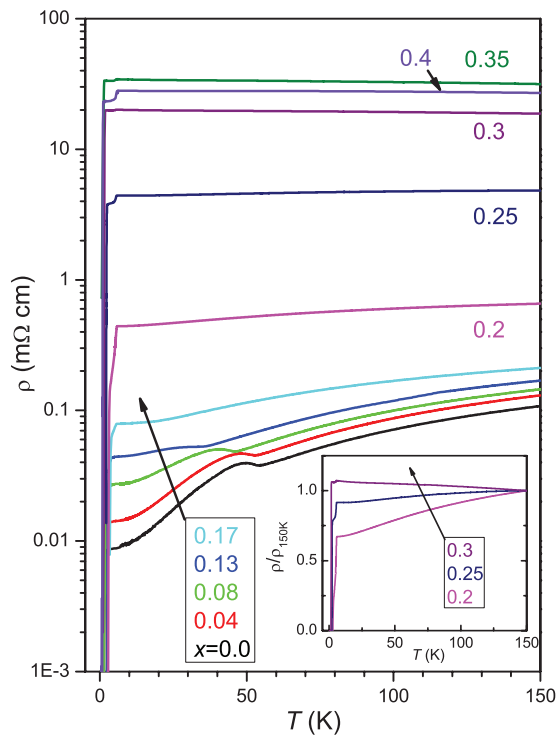


FIG. 2. (Color online) Temperature dependence of resistivity (in logarithmic scale) for the $\text{BaTi}_2(\text{Sb}_{1-x}\text{Bi}_x)_2\text{O}$ polycrystalline samples. The lower inset shows a sign change in the temperature coefficient of the normal-state resistivity around $x = 0.3$.

suppression of the DW state may be interpreted in terms of an increase of the c/a ratio associated with the negative chemical pressure.

In addition to the negative chemical pressure effect, the Bi doping induces disorder concomitantly. The low-temperature residual resistivity increases almost proportionally with x in the low-doping regime. This can be explained by conventional impurity scattering due to the Sb/Bi substitution disorder. For the high-doping samples, however, the absolute resistivity increases rapidly. The low- T resistivity increases by three orders of magnitude from $x = 0$ to $x = 0.3$. Furthermore, the temperature coefficient of resistivity (TCR) changes sign at $x \sim 0.3$, pointing to a metal-to-nonmetal (M-NM) transition. The origin of the M-NM transition is probably a disorder-induced Anderson localization,²⁴ since the Bi substitution takes place within the conducting $\text{Ti}_2\text{Sb}_2\text{O}$ layers. Besides, the increase of the c/a ratio reduces the dimensionality of the system, which may aggravate the disorder effect.

The detailed superconducting transitions in resistivity are displayed in Fig. 3. The parent compound shows a superconducting transition at $T_c^{\text{onset}} = 1.5$ K, basically consistent with the previous report.¹⁶ With Bi doping, T_c first increases steadily up to 3.7 K at $x = 0.17$, then decreases gradually for $x \geq 0.2$. A sharp superconducting transition at 0.8 K was still seen for the highest-doping sample with $x = 0.40$. Note that an obvious resistivity drop always appears at 5.7 K for the high-doping samples. These samples contain a remarkable impurity of bismuth (about 5% estimated from the relative intensities of the XRD peaks). This impurity could become

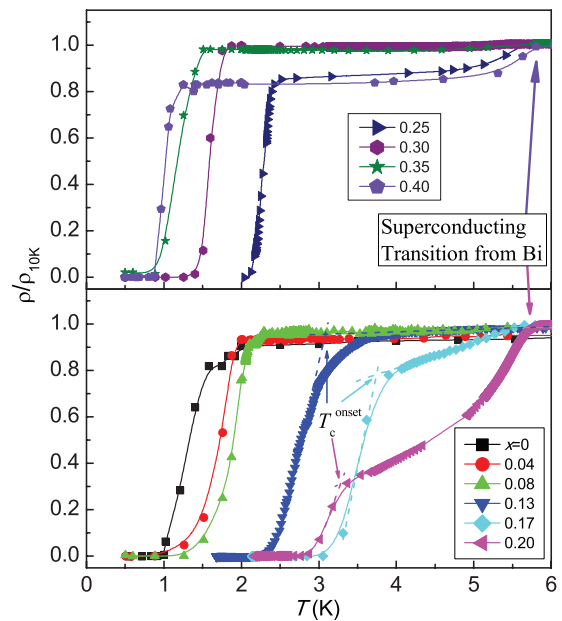


FIG. 3. (Color online) Superconducting transitions by the resistivity measurement in $\text{BaTi}_2(\text{Sb}_{1-x}\text{Bi}_x)_2\text{O}$. The definition of T_c^{onset} is marked on the plot.

superconducting owing to the quenchinglike process during the sample preparations.²⁵

Figure 4 shows the temperature dependence of the magnetic susceptibility $[\chi(T)]$ for the $\text{BaTi}_2(\text{Sb}_{1-x}\text{Bi}_x)_2\text{O}$ samples down to the lowest temperature available (~ 2 K). The magnetic susceptibility under $H = 10$ kOe indicates a DW anomaly (marked by arrows) below 55 K for the low-doping samples. The anomaly is weakened and T_{DW} decreases rapidly with Bi doping. No such anomaly can be detected for $x \geq 0.17$. These results are consistent with the above resistivity measurements shown in Fig. 2.

The superconducting diamagnetic transitions are also evident in the temperature scope. For $x = 0.04$ and 0.08 samples with a lower T_c , only superconducting onset transitions can be seen [the inset of Fig. 4(d)]. The transition temperature determined by the magnetic measurement (T_c^{mag}) agrees with the above resistivity measurement. Note that the diamagnetic transition at 5.7 K for the high-doping samples is again due to the superconducting transition from the Bi impurity. The $\chi(T)$ data in the ZFC mode show a magnetic shielding fraction of over 200% (because the theoretical density in the range of 6.0–6.7 g cm^{-3} was employed, and no demagnetization correction was made) for the samples with a higher T_c . The magnetic shielding signal is remarkably stronger than that of the parent compound¹⁶ and Na-doped $\text{BaTi}_2\text{Sb}_2\text{O}$.¹⁷ In contrast, a much lower diamagnetic signal (less than 1%) was measured in the FC mode. The vanishingly small magnetic repulsion suggests strong magnetic-flux trapping, which may be related to the Bi/Sb substitution disorder that could serve as a flux-pinning center.

Based on the above results, the electronic and superconducting phase diagram can be established in Fig. 5. The parent compound $\text{BaTi}_2\text{Sb}_2\text{O}$ undergoes both a DW ordering at 55 K and a superconducting transition at 1.5 K. The DW

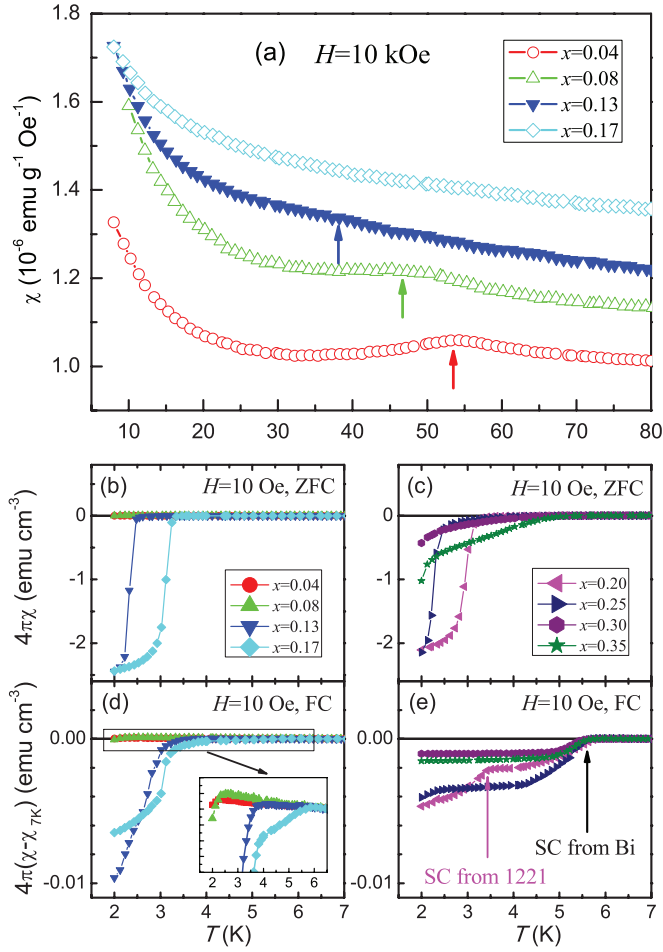


FIG. 4. (Color online) Temperature dependence of dc magnetic susceptibility (χ) for $\text{BaTi}_2(\text{Sb}_{1-x}\text{Bi}_x)_2\text{O}$. The upper plot (a) and the lower panels [(b)–(e)] show high- and low-field data, respectively. Note that the field-cooling (FC) data in (d) and (e) were subtracted by the χ value at 7 K for clarity. Owing to the limit of the lowest temperature available, only samples with $T_c > 2$ K show superconducting transitions.

state is suppressed by Bi doping, and it disappears for $x \geq 0.17$. Meanwhile the superconducting transition temperature is elevated to its maximum value $T_c = 3.7$ K at $x = 0.17$. A M–NM transition locates at $x \sim 0.3$. Nevertheless, SC does not vanish at the nonmetal side, indicating that the SC is robust to disorder.

Very recently, Yajima *et al.*²³ succeeded in synthesizing the oxybismide end member $\text{BaTi}_2\text{Bi}_2\text{O}$, and an enhanced T_c of 4.6 K with no DW anomaly was reported. This result is consistent with the case of lower-doping ($x \leq 0.17$) $\text{BaTi}_2(\text{Sb}_{1-x}\text{Bi}_x)_2\text{O}$, which can be understood in terms of the lattice expansion and distortion associated with negative chemical pressure (see below). For the higher-doping ($x \geq 0.2$) scenario, the disorder effect induces Anderson localization and suppresses T_c . Therefore, for the Bi-rich ($0.5 < x < 1$) regime, we anticipate that T_c would decrease monotonically if Bi is partially substituted by Sb in $\text{BaTi}_2\text{Bi}_2\text{O}$.

Therefore, Bi doping in the 1221 system brings about two effects: lattice expansion and disorder. The former can

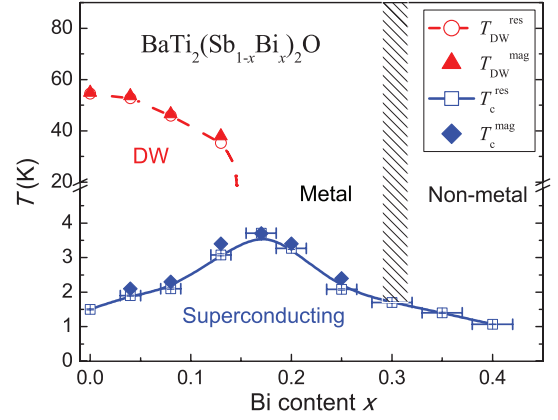


FIG. 5. (Color online) Electronic and superconducting phase diagram of $\text{BaTi}_2(\text{Sb}_{1-x}\text{Bi}_x)_2\text{O}$. DW refers to the spin- or charge-density wave state. The phase boundaries are determined by both resistivity (T^{res}) and magnetic susceptibility (T^{mag}) measurements. Note that the vertical axis was broken from 5 to 20 K in order to show the related phases clearly.

be viewed as a consequence of negative pressure, which also leads to the structural distortion of the $\text{Ti}_2\text{Sb}_2\text{O}$ layers. The structural distortion of the $\text{Ti}_2\text{Sb}_2\text{O}$ layers, measured by the c/a ratio, is closely related to the DW state and possibly to SC also. The negative chemical pressure increases the c/a ratio, hence it decreases T_{DW} and correspondingly increases T_c . However, the maximum T_c is still about 1 and 2 K lower than those of $\text{BaTi}_2\text{Bi}_2\text{O}$ (Ref. 23) and the Na-doped $\text{BaTi}_2\text{Sb}_2\text{O}$.¹⁷ This implies that Bi/Sb substitution disorder plays a role. In the high-doping region, such disorder leads to an Anderson localization that is responsible for the observed M–NM transition. Surprisingly, SC still appears when the normal state shows nonmetallic behaviors (negative TCR and relatively high resistivity). This fact suggests a possible realization of “fractal superconductivity” near the localization threshold in the present system.²⁶ This interesting issue deserves future explorations.

In summary, we have investigated an isovalent substitution effect on SC and CDW/SDW in the $\text{BaTi}_2(\text{Sb}_{1-x}\text{Bi}_x)_2\text{O}$ system. Bi doping induces negative chemical pressure which not only expands but also distorts the lattice. It was found that the CDW/SDW ordering was completely suppressed at $x = 0.17$, and concomitantly the superconducting transition temperature was elevated to a maximum T_c of 3.7 K. A metal-to-nonmetal transition at $x \sim 0.3$ was observed, which is interpreted by Anderson localization due to Bi/Sb substitution disorder. Interestingly, such disorder does not kill the superconductivity. These results supply some useful clues to further study the nature of the CDW/SDW phase and its relations to superconductivity in $\text{BaTi}_2\text{Sb}_2\text{O}$ -related systems.

This work is supported by the NSF of China (No. 11190023), the National Basic Research Program of China (No. 2010CB923003 and No. 2011CBA00103), and the Fundamental Research Funds for the Central Universities of China.

*ghcao@zju.edu.cn

- ¹For related reviews, see J. A. Wilson, F. J. Di Salvo, and S. Mahajan, *Adv. Phys.* **24**, 117 (1975); A. M. Gabovich, A. I. Voitenko, and M. Ausloos, *Phys. Rep.* **367**, 583 (2002).
- ²J. Zhao, Q. Huang, C. de la Cruz, S. L. Li, J. W. Lynn, Y. Chen, M. A. Green, G. F. Chen, G. Li, Z. Li, J. L. Luo, N. L. Wang, and Pengcheng Dai, *Nat. Mater.* **7**, 953 (2008).
- ³H. Chen, Y. Ren, Y. Qiu, W. Bao, R. H. Liu, G. Wu, T. Wu, Y. L. Xie, X. F. Wang, Q. Huang, and X. H. Chen, *Europhys. Lett.* **85**, 17006 (2009).
- ⁴D. C. Johnston, *Adv. Phys.* **59**, 803 (2010); J. Paglione and R. L. Greene, *Nat. Phys.* **6**, 645 (2010); G. R. Stewart, *Rev. Mod. Phys.* **83**, 1589 (2011).
- ⁵A. Adam and H.-U. Schuster, *Z. Anorg. Allg. Chem.* **584**, 150 (1990).
- ⁶E. A. Axtell III, T. Ozawa, S. M. Kauzlarich, and R. R. P. Singh, *J. Solid State Chem.* **134**, 423 (1997).
- ⁷T. C. Ozawa, S. M. Kauzlarich, M. Bieringer, and J. E. Greedan, *Chem. Mater.* **13**, 1804 (2001).
- ⁸T. C. Ozawa and S. M. Kauzlarich, *Sci. Technol. Adv. Mater.* **9**, 033003 (2008).
- ⁹R. H. Liu, D. Tan, Y. A. Song, Q. J. Li, Y. J. Yan, J. J. Ying, Y. L. Xie, X. F. Wang, and X. H. Chen, *Phys. Rev. B* **80**, 144516 (2009).
- ¹⁰X. F. Wang, Y. J. Yan, J. J. Ying, J. Q. Li, M. Zhang, N. Xu, and X. H. Chen, *J. Phys.: Condens. Matter* **22**, 075702 (2010).
- ¹¹R. H. Liu, Y. A. Song, Q. J. Li, J. J. Ying, Y. J. Yan, Y. He, and X. H. Chen, *Chem. Mater.* **22**, 1503 (2010).
- ¹²W. E. Pickett, *Phys. Rev. B* **58**, 4335 (1998).
- ¹³F. F. de Biani, P. Alemany, and E. Canadell, *Inorg. Chem.* **37**, 5807 (1998).
- ¹⁴R. R. P. Singh, O. A. Starykh, and P. J. Freitas, *J. Appl. Phys.* **83**, 7387 (1998).
- ¹⁵Y. L. Sun, H. Jiang, H. F. Zhai, J. K. Bao, W. H. Jiao, Q. Tao, C. Y. Shen, Y. W. Zeng, Z. A. Xu, and G. H. Cao, *J. Am. Chem. Soc.* **134**, 12893 (2012).
- ¹⁶T. Yajima, K. Nakano, F. Takeiri, T. Ono, Y. Hosokoshi, Y. Matsushita, J. Heister, Y. Kobayashi, and H. Kageyama, *J. Phys. Soc. Jpn.* **81**, 103706 (2012).
- ¹⁷P. Doan, M. Gooch, Z. Tang, B. Lorenz, A. Moeller, J. Tapp, P. C. W. Chu, and A. M. Guloy, *J. Am. Chem. Soc.* **134**, 16520 (2012).
- ¹⁸T. C. Ozawa, T. Pantoja, E. A. Axtell III, S. M. Kauzlarich, J. E. Greedan, M. Bieringer, and J. W. Richardson, Jr., *J. Solid State Chem.* **153**, 275 (2000).
- ¹⁹H. Jiang, Y. L. Sun, J. H. Dai, G. H. Cao, and C. Cao, *arXiv:1207.6705*.
- ²⁰D. J. Singh, *New J. Phys.* **14**, 123003 (2012).
- ²¹X. W. Yan and Z. Y. Lu, *arXiv:1210.3481*.
- ²²A. Subedi, *Phys. Rev. B* **87**, 054506 (2013).
- ²³After completion of our experiments, we became aware of a recent report on the superconductivity in BaTi₂Bi₂O [T. Yajima *et al.*, *J. Phys. Soc. Jpn.* **82**, 013703 (2013)]. The result is consistent with one of our conclusions, i.e., the lattice expansion is favored for superconductivity.
- ²⁴P. W. Anderson, *Phys. Rev.* **109**, 1492 (1958).
- ²⁵Metal Bi becomes superconducting at about 6 K, in the form of amorphous thin films [J. S. Shier and D. M. Ginsberg, *Phys. Rev.* **147**, 384 (1966)]. This noncrystallinelike Bi forms reasonably during the sample cooling from a very high sintering temperature of 1323 K.
- ²⁶M. V. Feigel'man, L. B. Ioffe, V. E. Kravtsov, and E. Cuevas, *Ann. Phys.* **325**, 1390 (2010).